

## Electronic Supplementary Information (ESI)

### Substrate-free Mo<sub>2</sub>C-based electrocatalyst by facile glucose-blowing for efficient hydrogen production

Xiao Li,<sup>ac</sup> Xiao-Li Hu,<sup>\*ac</sup> Xin-Long Wang,<sup>\*bc</sup> Qing Qing Pan,<sup>ac</sup> Lei Liu<sup>a</sup> and Zhong-Min Su<sup>\*abc</sup>

<sup>a</sup>School of Chemistry and Environmental Engineering, Changchun University of Science and Technology, Changchun 130022, China. Email: huxiaoli1113@cust.edu.cn.

<sup>b</sup>Institute of Functional Material Chemistry, Local United Engineering Lab for Power Battery, Northeast Normal University, Changchun, 130024, China. Email: zmsu@nenu.edu.cn.

<sup>c</sup>Jilin Provincial Science and Technology Innovation Center of Optical Materials and Chemistry, Changchun. 130022, China.

## Materials and method

Commercial chemicals used in reactions were purchased without purification. PXRD patterns were gathered by a Siemens D5005 diffractometer with Cu-K $\alpha$  ( $\lambda = 1.5418\text{\AA}$ ) radiation ranging from 3° to 80° at 293K with a rate of 5 min<sup>-1</sup>. A JY Labram HR 800 is carried out for the Raman spectra. A SU8000 ESEM FEG microscope was utilized to obtain the interrelated energy dispersive X-ray detector (EDX) spectra. The N<sub>2</sub> sorption tests were measured on automatic volumetric adsorption equipment (Belsorp mini II). The TEM was accomplished on a JEOL-2100F transmission electron microscope.

### Preparation of Gb-Mo<sub>2</sub>C@PC

0.5g of PMo<sub>12</sub>, 0.5g NH<sub>4</sub>Cl and 0.5g glucose with the mass ratio of 1:1:1 was ground well for 30min. Other ratios also mean mass ratios. The resulting mixture was put into a tube furnace with the ramping rate at 5 °C min<sup>-1</sup>, subsequently, maintained at 900 °C for 2 h and naturally cooled down to 25 °C under N<sub>2</sub> flow. Hereafter, the samples were soaked in 2 M HCl under an ultrasonic condition for 30 min to remove the unstable composition. Finally, copious amount of deionized water was used to wash the product until the solution is about neutral. The samples were dried at 80 °C overnight before use.

### Electrochemical measurements

We use an electrochemical workstation (CHI 660e, China) to conduct the electrochemical measurements with a three-electrode system. The working electrode is a GC electrode (d = 3mm), a graphite rod is the counter electrode and the reference electrode is an Ag/AgCl electrode. For Gb-Mo<sub>2</sub>C@PC, 20 mg of the samples were dispersed in the mixture of 100  $\mu$ L of 0.5wt% Nafion solution, 1 mL of water and 0.8 mL of ethanol, followed by ultrasonication for 30 min to make an even suspension. After ultrasonication, 5 $\mu$ L of the suspension was pipetted onto the GC electrode. Then, the working electrode was dried naturally under ambient temperature. The final mass loading of the catalysts is about 0.74 mg cm<sup>-2</sup>. Commercial Pt/C electrocatalyst with same preparation was conducted with the same loading with Gb-Mo<sub>2</sub>C@PC.

LSV curves were measured deaerated with nitrogen with a scan rate of 5 mV s<sup>-1</sup> in 0.5 M H<sub>2</sub>SO<sub>4</sub> and 1 M KOH aqueous solutions at 25 °C prior to the HER. The catalysts were activated using 20 cyclic voltammetry scans with a scan rate of 100 mV s<sup>-1</sup> before recording the electrochemical performance. All the potentials were referenced to a reversible hydrogen electrode (RHE) computed by the Nernst equation:  $E_{\text{RHE}} = E_{\text{Ag/AgCl}} + 0.059\text{pH} + 0.197\text{V}$ . All data displayed here was treated without iR compensation.

The CV measurements were taken with scan rates of 10, 30, 50, 80, 100, 150, 200 mV s<sup>-1</sup> between 0.10V and 0.30V, respectively. EIS spectra were operated on a PARSTAT 2273 electrochemical system (Princeton Applied Research Instrumentation, USA) with the frequencies in the range of 0.1-100 000 Hz at an amplitude of 5 mV.

## 1. Physical characterization of Gb-Mo<sub>2</sub>C@PC

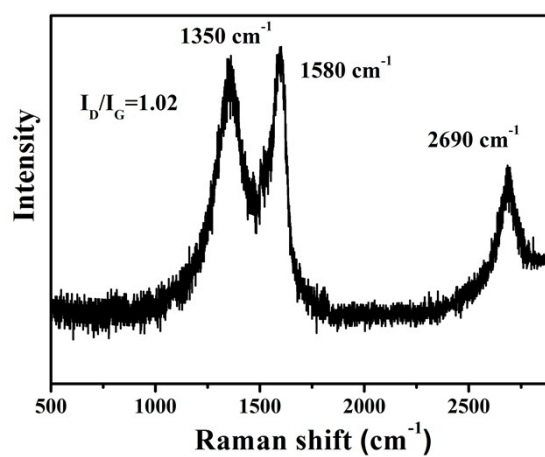


Fig. S1 Raman spectrum of Gb-Mo<sub>2</sub>C@PC with  $I_G/I_D = 1.02$ , indicating the partial graphitization at 900 °C. The presence of the 2D peak at 2690 cm<sup>-1</sup> further confirms the partially graphitic species in the electrocatalyst.

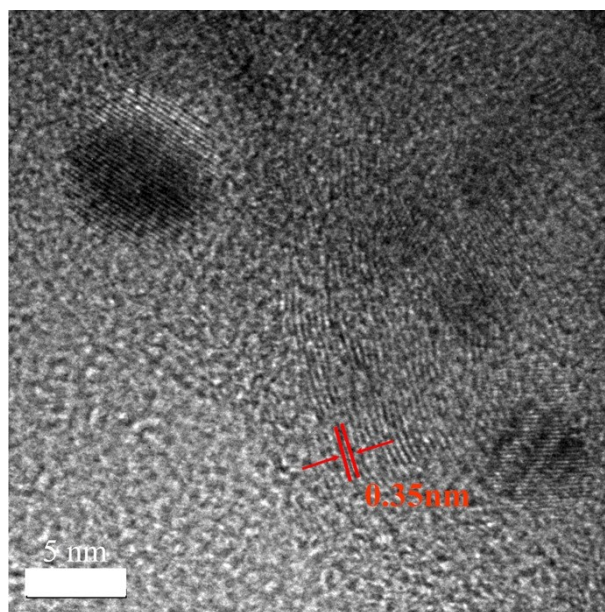


Fig. S2 HRTEM images of Gb-Mo<sub>2</sub>C@PC (the d-spacing distance of multiple graphene layers).

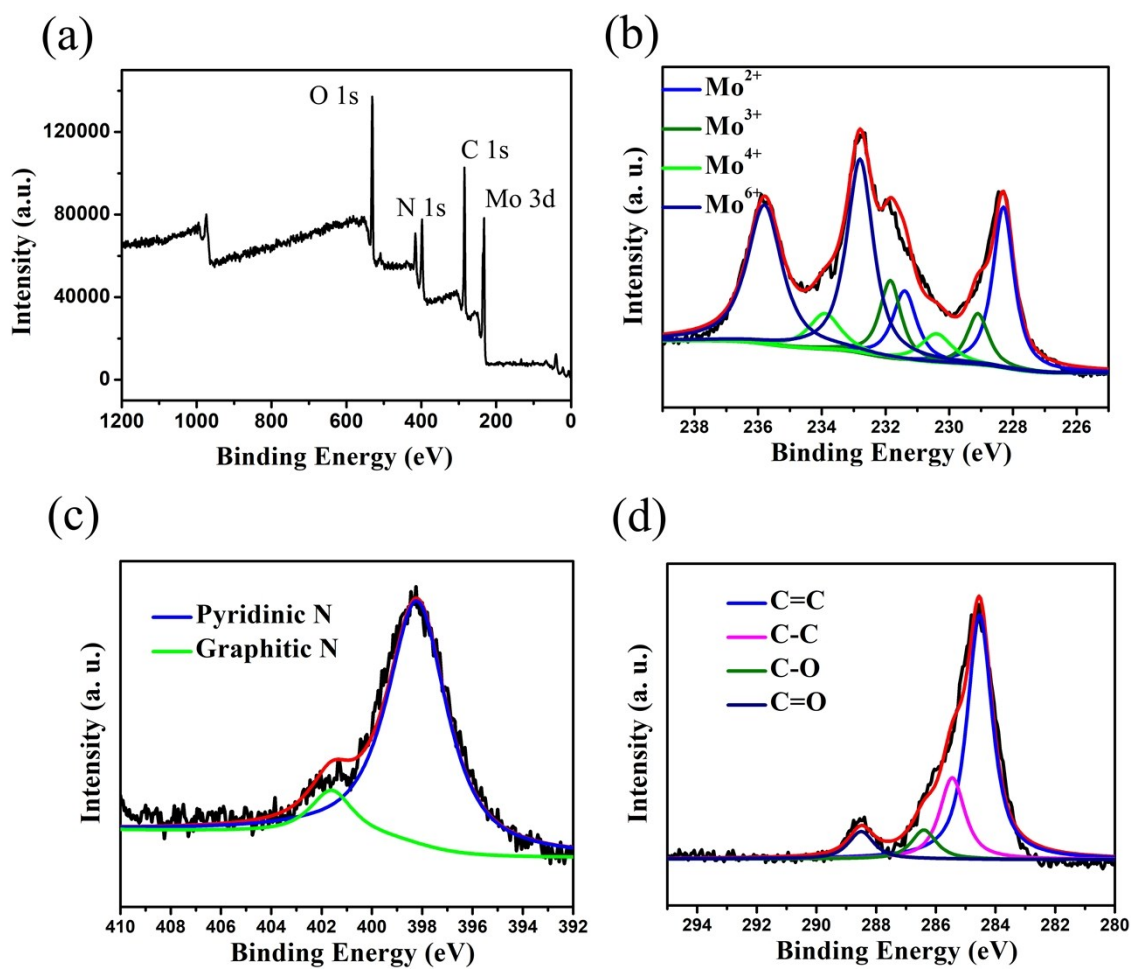


Fig. S3 X-ray photoelectron spectra of Gb-Mo<sub>2</sub>C@PC.

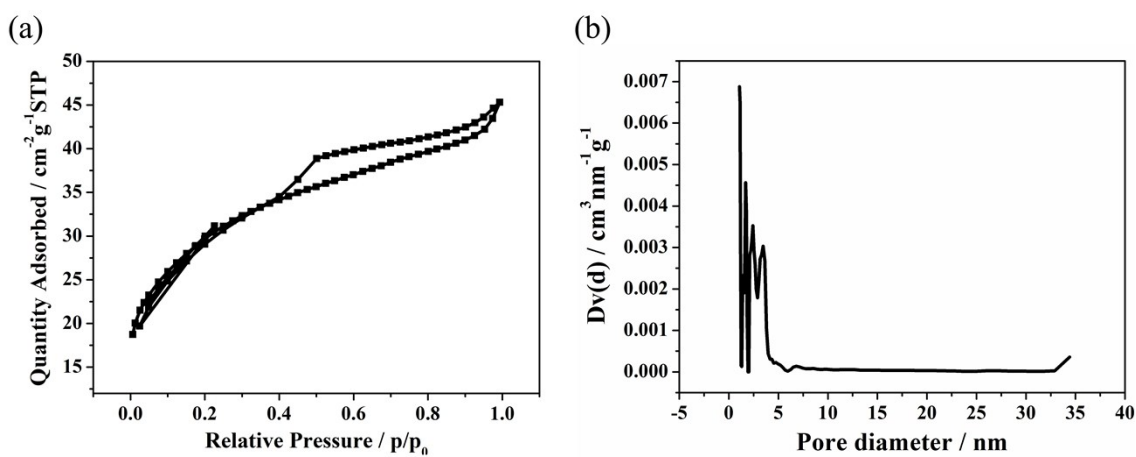


Fig. S4 (a) N<sub>2</sub> adsorption-desorption isotherms. (b) The pore-size distribution of Gb-Mo<sub>2</sub>C@PC.

## 2. Additional electrochemical experiment of Gb-Mo<sub>2</sub>C@PC

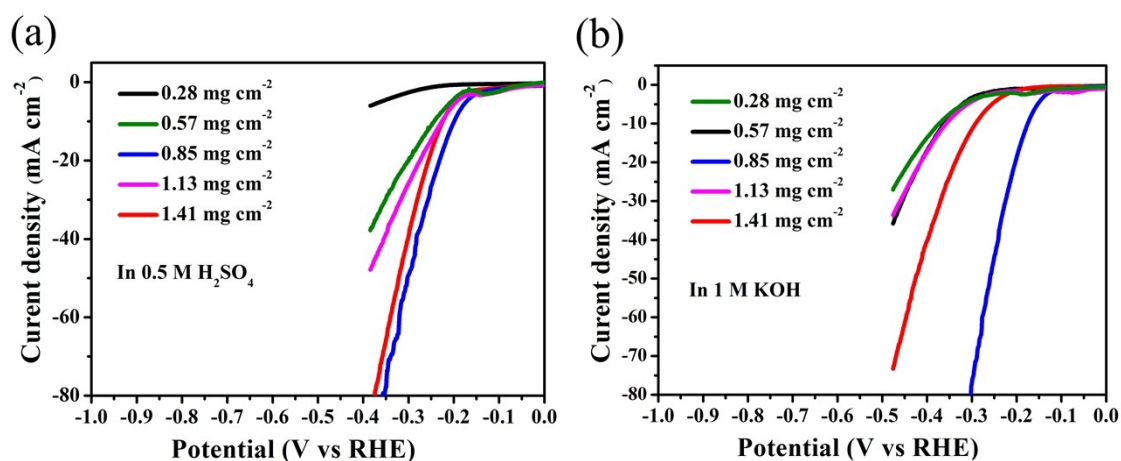


Fig. S5 (a) and (b) Polarization curves of Gb-Mo<sub>2</sub>C@PC with different mass loadings on a glassy carbon electrode in 0.5M H<sub>2</sub>SO<sub>4</sub> and 1M KOH.

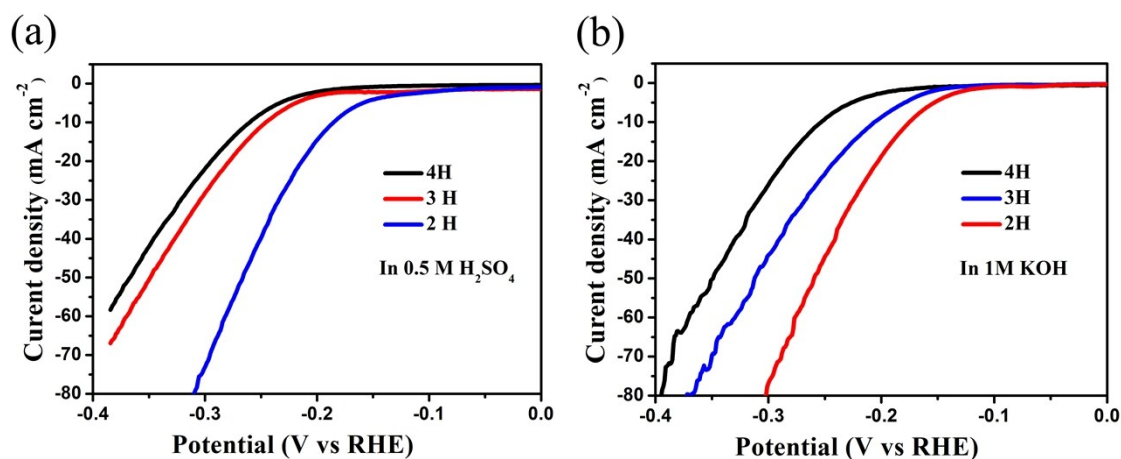


Fig.S6 (a) and (b) Polarization curves of Gb-Mo<sub>2</sub>C@PC with different carburizing time at 700 °C on a glassy carbon electrode in 0.5M H<sub>2</sub>SO<sub>4</sub> and 1M KOH.

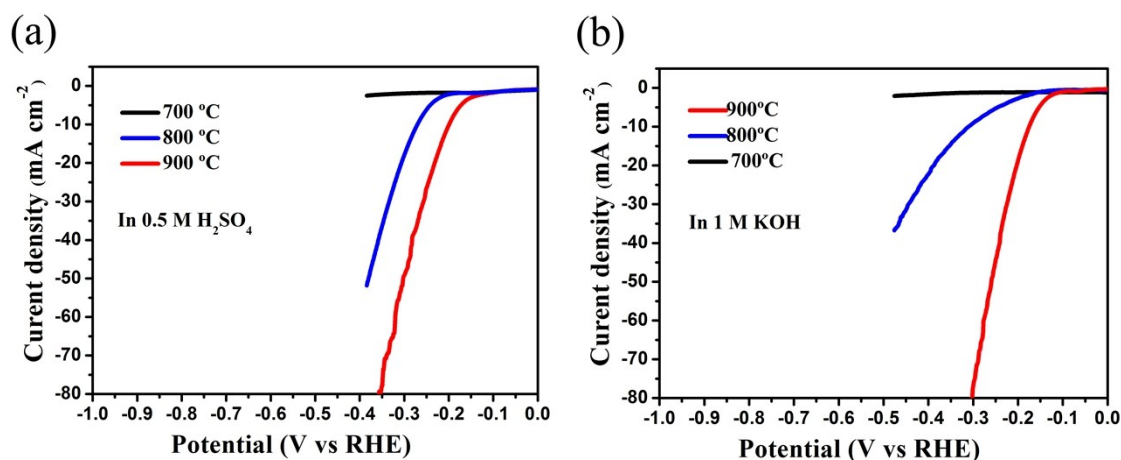


Fig.S7 (a) and (b) Polarization curves of Gb-Mo<sub>2</sub>C@PC with different carburizing temperatures on a glassy carbon electrode in 0.5M H<sub>2</sub>SO<sub>4</sub> and 1M KOH.

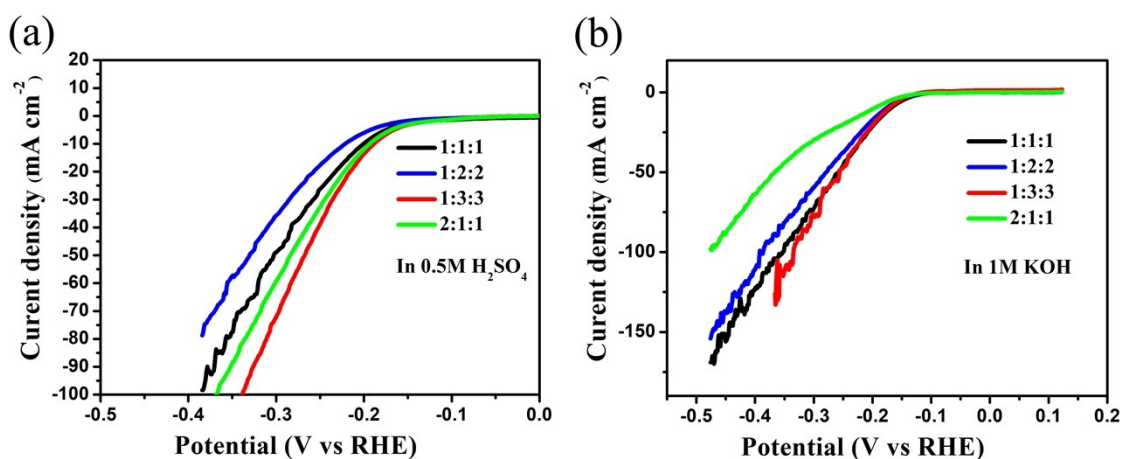
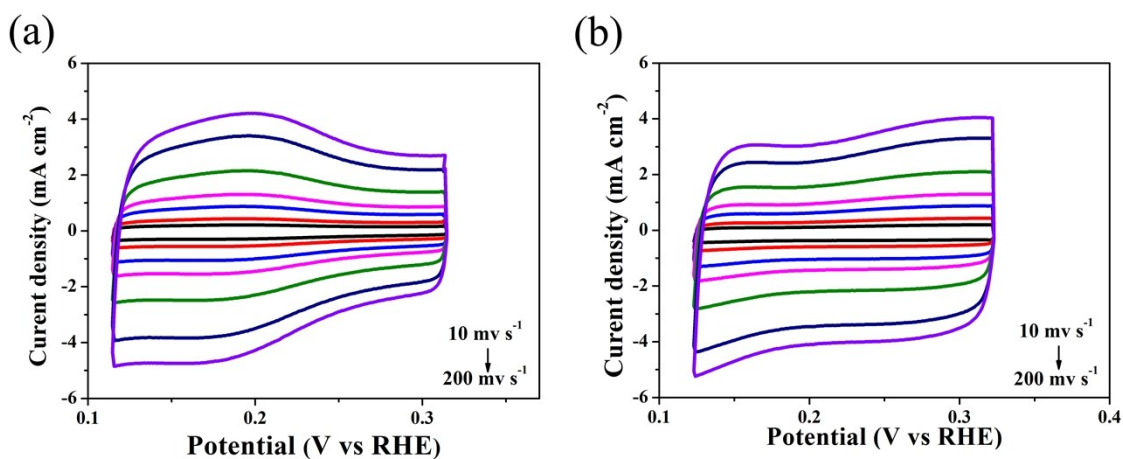


Fig.S8 (a) and (b) Polarization curves of **Gb-Mo<sub>2</sub>C@PC** with different ratios on a glassy carbon electrode in 0.5M H<sub>2</sub>SO<sub>4</sub> and 1M KOH.



(c)

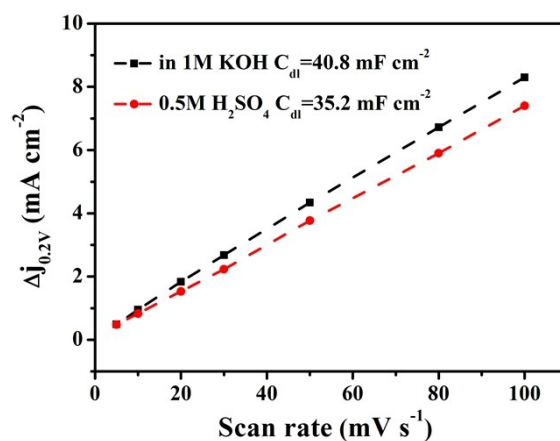


Fig.S9 Cyclic voltammograms (CVs) of **Gb-Mo<sub>2</sub>C@PC** in 0.5 M H<sub>2</sub>SO<sub>4</sub> (a) and 1 M KOH (b); Liner fitting of  $\Delta j$  ( $\Delta j = j_a - j_c$ ) vs. scan rates at a given overpotential of +0.35 V vs. RHE in 0.5M H<sub>2</sub>SO<sub>4</sub> and in 1M KOH (c), respectively.  $j_a$  represents the anodic current density and  $j_c$  represents the cathodic current density.



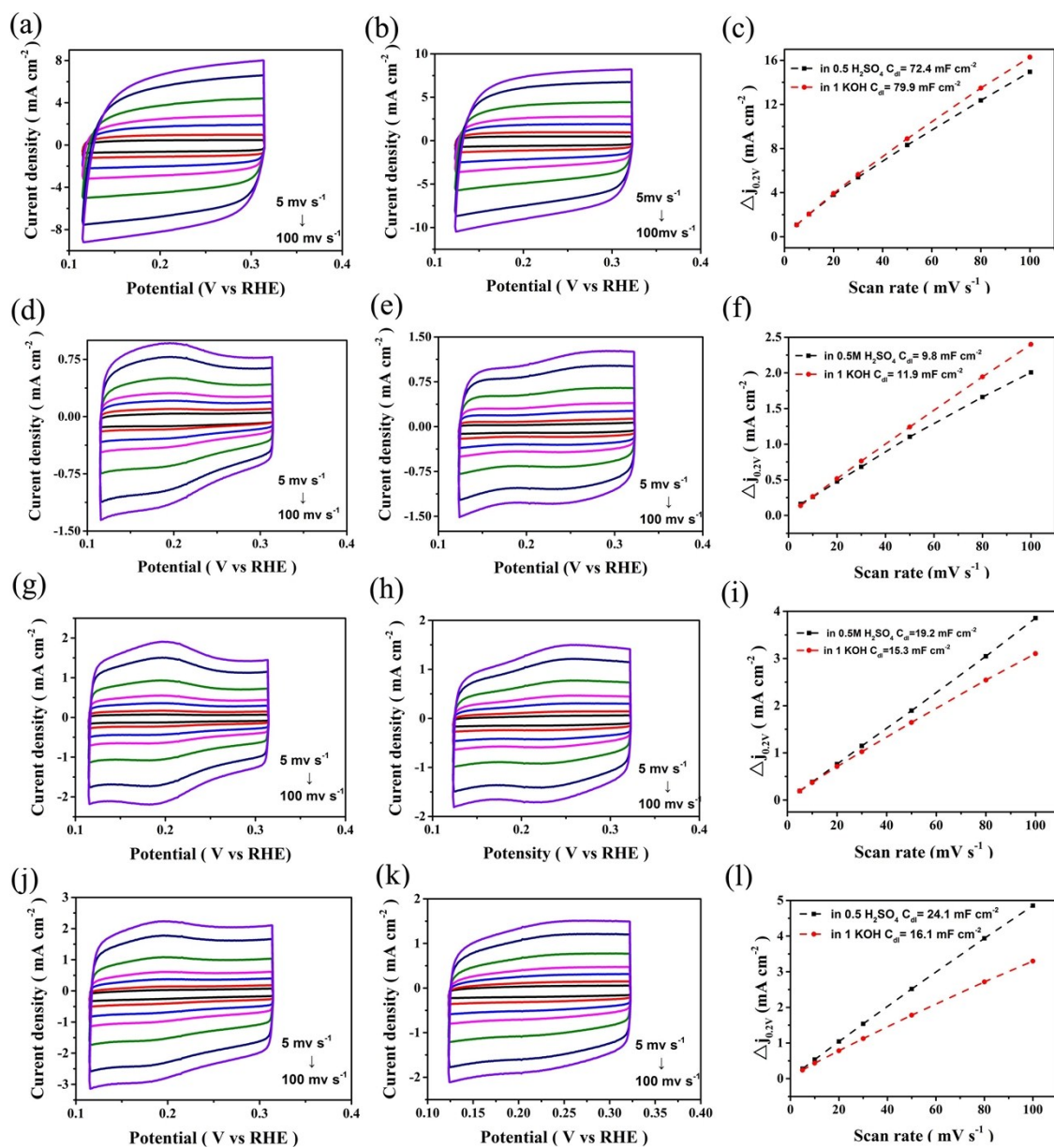


Fig.S10 Cyclic voltammograms (CVs) of other control samples (a-c, NC; d-f, 1:1:1; g-i, 1:2:2; j-l, 2:1:1) with different mass ratios in 0.5 M H<sub>2</sub>SO<sub>4</sub> and 1 M KOH (b); Liner fitting of  $\Delta j$  ( $\Delta j = j_a - j_c$ ) vs. scan rates at a given overpotential of + 0.35 V vs. RHE in 0.5M H<sub>2</sub>SO<sub>4</sub> and in 1M KOH, respectively.  $j_a$  represents the anodic current density and  $j_c$  represents the cathodic current density.



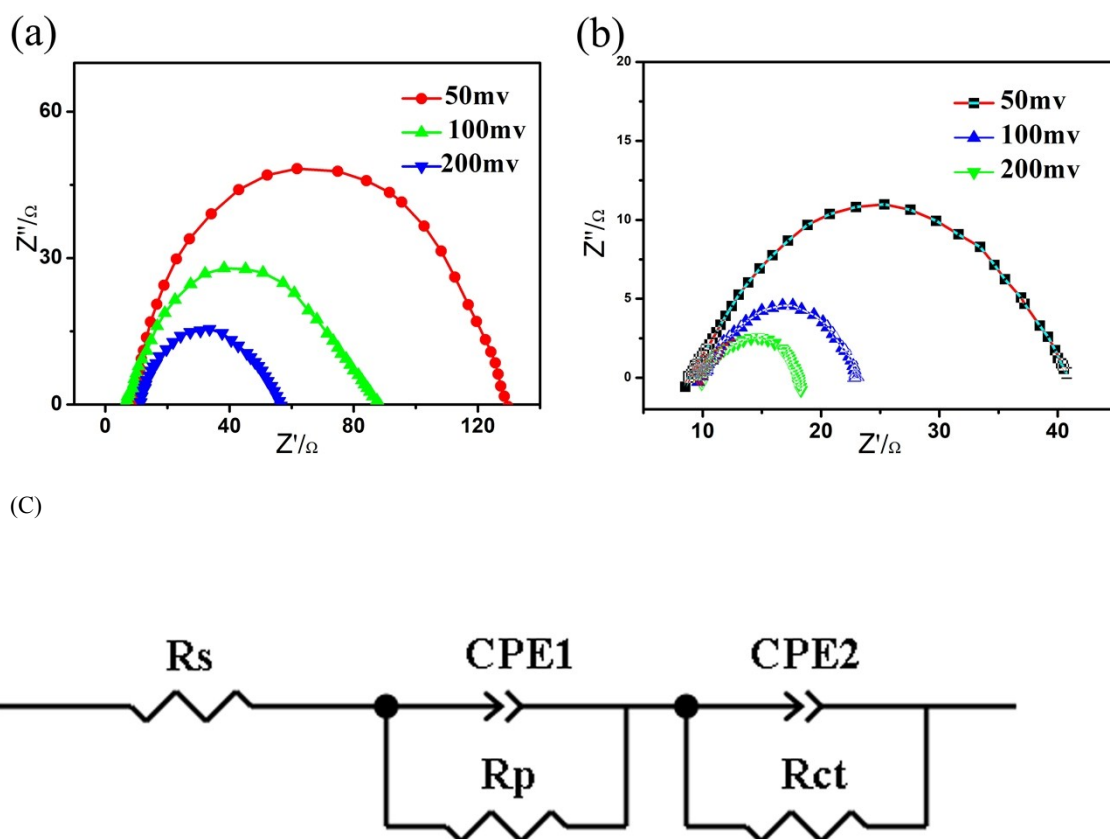


Fig. S11 Nyquist plots of electrochemical impedance spectra (EIS) of **Gb-Mo<sub>2</sub>C@PC** obtained in 0.5 M H<sub>2</sub>SO<sub>4</sub> (a) and in 1 M KOH aqueous solutions. (c) Two-time constant model, including a series resistance ( $R_s$ ), two constant phase elements (CPE1 and CPE2), resistance corresponding to surface porosity ( $R_p$ ), and charge transfer resistance corresponding to HER process ( $R_{ct}$ ).

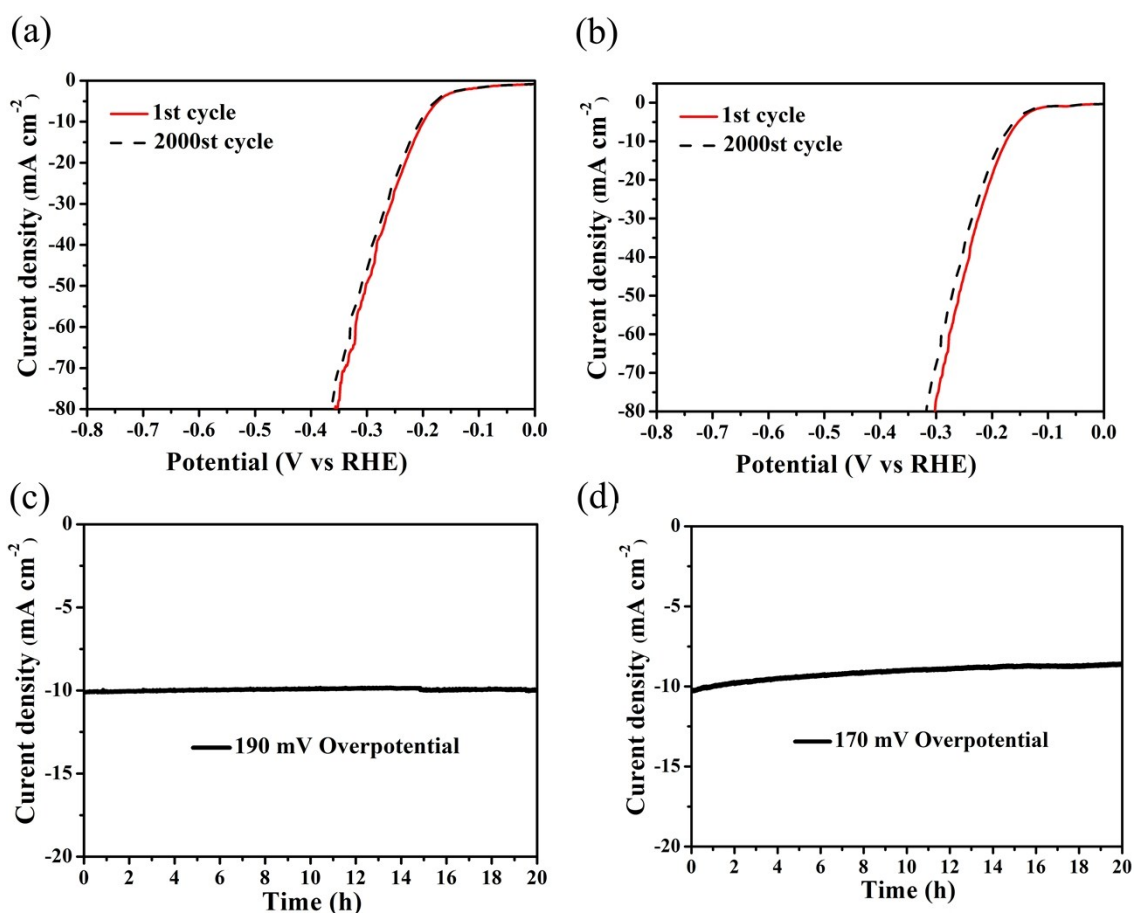


Fig. S12 (a) and (b) Polarization curves after continuous potential sweeps at  $50 \text{ mV s}^{-1}$  in  $0.5 \text{ M H}_2\text{SO}_4$  and  $1 \text{ M KOH}$ . (c) and (d) Time-dependent current density curves under  $\eta = 190 \text{ mV}$  and  $170 \text{ mV}$  in  $0.5 \text{ M H}_2\text{SO}_4$  and  $1 \text{ M KOH}$ .

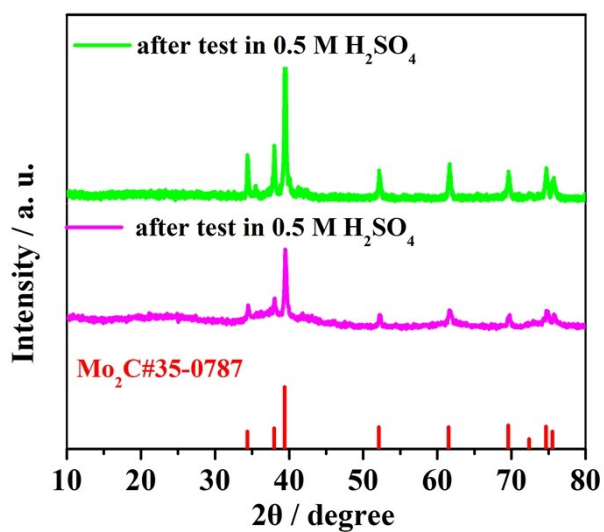


Figure S13. XRD patterns of Gb-Mo<sub>2</sub>C@PC after stability test in  $0.5 \text{ M H}_2\text{SO}_4$  and  $1 \text{ M KOH}$ .

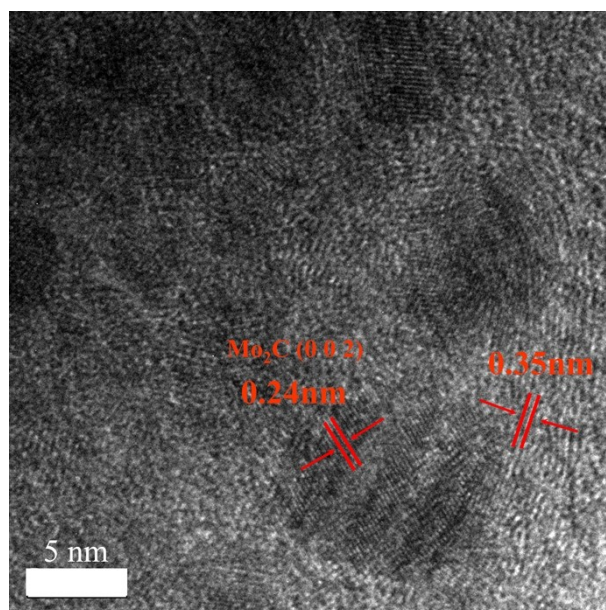


Figure S14. TEM image of **Gb-Mo<sub>2</sub>C@PC** after stability test in 0.5 M H<sub>2</sub>SO<sub>4</sub>.

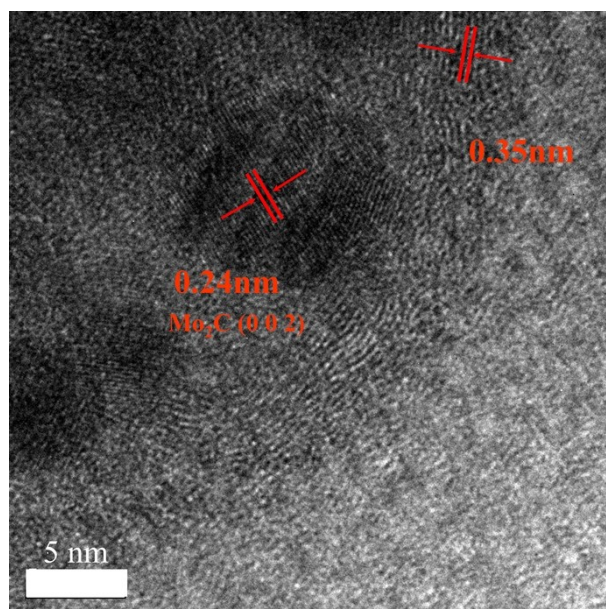


Figure S15. TEM image of **Gb-Mo<sub>2</sub>C@PC** after stability test in 1 M KOH.

### 3. Comparison of HER parameters of different non-Pt catalysts.

Table S1 Comparison for HER activity in acidic solutions for **Gb-Mo<sub>2</sub>C@PC** with other electrocatalysts.

Catalysts	Loading mass (mg cm <sup>-2</sup> )	$\eta_{10}/mV$	Tafel slope (mV decade <sup>-1</sup> )	Ref.
<b>Gb-Mo<sub>2</sub>C@PC</b>	0.15	188	76	This work
MCC-3	1	175	66	Small 2017, 1701246
Mo <sub>2</sub> C NPs	0.102	198	56	J. Mater. Chem. A. 2015, 3, 8361
Co <sub>0.6</sub> Mo <sub>1.4</sub> N <sub>2</sub>	0.24	200	/	J. Am. Chem. Soc. 2013, 135, 19186
Mo <sub>2</sub> C/C	0.84	135	75.1	J. Mater. Chem. A. 2017, 5, 4879
Mo <sub>2</sub> C-GNR	0.57	152	69	ACS Nano 2017,11,384
Mo <sub>2</sub> C-carbon nanocomposites	0.25	147	110-235	J. Mater. Chem. A., 2014, 2, 10548-10556.
Mo <sub>2</sub> C@N-CNFs	/	192	70	Npg Asia Mater. 2016, 8, e288
Mo <sub>2</sub> C Nanoparticles Decorated Graphitic Carbon Sheets	0.36	210	62.6	ACS Catal. 2014, 4, 2658
Mo <sub>2</sub> C and MoB microparticles	1.4-2.5	~225	55~56	Angew. Chem. Int. Ed. 2012, 124, 12875

Table S2 Comparison for HER activity in basic solutions for **Gb-Mo<sub>2</sub>C@PC** with other electrocatalysts.

Catalysts	Loading mass (mg cm <sup>-2</sup> )	$\eta_{10}/\text{mV}$	Tafel slope (mV decade <sup>-1</sup> )	Ref.
<b>Gb-Mo<sub>2</sub>C@PC</b>	0.15	169	45	This work
Mo <sub>2</sub> C NPs	0.102	176	58	J. Mater. Chem. A. 2015, 3, 8361
Porous MoC <sub>x</sub> nano-octahedrons	0.8	151	59	Nat. Commun. 2015, 6, 6512
Mo <sub>2</sub> C –GNR	0.57	121	59	ACS Nano 2017, 11, 384
CoO <sub>x</sub> @CN	0.12	232	115	J. Am. Chem. Soc. 2015, 137, 2688
Mo <sub>2</sub> C-NCNT	3	257	71	J. Mater. Chem. A. 2015, 3, 5783
Mo <sub>2</sub> C	0.009	270	67	J. Am. Chem. Soc. 2015, 137, 7035
Mo <sub>2</sub> C	0.8	190	54	Angew. Chem. Int. Ed. 2012, 51, 12703
Mo <sub>2</sub> C/NCF	0.28	100	65	ACS Nano 2016, 10, 11337
NiMo <sub>2</sub> C@C	0.15	181	84	J. Mater. Chem. A. 2017, 5, 5000